ELSEVIER

Journal of Nuclear Materials 307–311 (2002) 1375–1379

journal of nuclear materials

www.elsevier.com/locate/jnucmat

Steam oxidation of PFC materials for advanced tokamaks

R.A. Anderl [a,*], R.J. Pawelko [a], G.R. Smolik [a], G. Piazza [b], F. Scaffidi-Argentina [c], L.L. Snead [d]

[a] *Idaho National Engineering and Environmental Laboratory, P.O. Box 1625, Idaho Falls, ID 83415-7113, USA*
[b] *Forschungszentrum Karlsruhe, IKET, Postfach 3640, D-76021 Karlsruhe, Germany*
[c] *EFDA Close Support Unit-Culham, Culham Science Center, Abingdon OX14 3DB, UK*
[d] *Oak Ridge National Laboratory, P.O. Box 2008, Oak Ridge, TN 37831-6087, USA*

Abstract

Steam chemical reactivity experiments were conducted for several ITER-like tokamak plasma-facing-component (PFC) materials: NB31 and NS31 carbon fiber composites (CFCs), W–1%La, DShG-200 Be, and Be (S65C and Kawecki PO Ductile Be) specimens irradiated to fast neutron fluences ranging from 5×10^{19} to 1×10^{21} n/cm^2. Experiments were performed at 800–1100 °C for CFC, 550–1000 °C for W–1%La, 500–900 °C for unirradiated Be, and 600–800 °C for irradiated Be. Average hydrogen generation rates are presented for these new measurements as a function of temperature, and the results are compared to previous studies on similar materials. In general, the new results extend the temperature and material range from previous studies, are consistent with previous work, and provide Arrhenius-type hydrogen generation expressions useful for safety assessment calculations. Little irradiation influence on oxidation behavior was observed for Be irradiated to 1×10^{21} n/cm^2, whereas significant influence was observed in previous tests on Be irradiated to 5×10^{22} n/cm^2.

1. Introduction

Evaluation of the safety hazards for advanced tokamaks includes an assessment of the failures of plasma-facing-component (PFC) materials due to accident scenarios, e.g. a loss of coolant accident (LOCA) that injects steam into the torus vacuum vessel. Steam ingress can generate substantial quantities of hydrogen via steam interactions with the proposed PFC materials. Assessment of such LOCAs typically requires experimentally derived chemical reactivity data for the PFC materials.

The purpose of this paper is to present the results of new measurements for carbon fiber composites (CFCs) NS31 and NB31 [1], tungsten alloy W–1%La, and DShG-200 beryllium, and to examine the impact of neutron irradiation on steam oxidation behavior of Be. These results are compared to previous steam chemical reactivity data for graphite and CFC composites [2–6], tungsten alloys [7,8], unirradiated Be [9–13], and irradiated Be [14,15].

2. Experimental details

2.1. Sample description and characterization

NS31 and NB31 are advanced 3D carbon fiber composites developed by SEP (Société Européenne de Propulsion) and Dunlop for high thermal conductivity applications [1]. NS31 is produced similarly to NB31 except it includes a final infiltration of liquid silicon (about 8–10 at.% Si) resulting in a product with higher density and lower porosity. For our steam oxidation experiments, samples with nominal dimensions (25 mm long, 8 mm wide, 3–4 mm thick) were cut from blocks of each CFC. Based on mass and dimensional

* Corresponding author. Tel.: +1-208 533 4153; fax: +1-208 533 4207.
E-mail address: raa@inel.gov (R.A. Anderl).

0022-3115/02/$ - see front matter
PII: S0022-3115(02)01067-X

measurements we computed average densities of 2.13 g/cc (±2%) for NS31 and 1.96 g/cc (±1%) for NB31. Similar density values were obtained from water immersion density measurements that also provided open porosity values of (1.8 ± 0.4)% for NS31 and (6.2 ± 0.4)% for NB31. BET specific surface areas [16], measured for each CFC test sample using a Kr gas adsorption technique, were 0.15 m^2/g (±14%) for NS31 and 0.15 m^2/g (±7%) for NB31. For each CFC test sample, the BET surface area was ~330 times the geometric surface area. Optical and scanning electron microscopy and energy-dispersive X-ray spectrometry measurements revealed that the microstructures of NS31 and NB31 CFC were similar except for one major difference. Voids and substantial porosity were observed in NB31, whereas, the porosity of NS31 was filled with Si, a fraction of which was converted to SiC during processing at elevated temperatures. However, microcracks along material interfaces were still present in the NS31 material and resulted in similar BET values.

Tungsten alloy specimens with nominal dimensions (12 mm long, 10 mm wide, 5 mm thick) were cut from a block of W–1%La tungsten alloy (includes 1–wt% La_2O_3) fabricated by Plansee for ITER applications. Final sample surface finish was established by mechanical polishing with 600-grit sandpaper. Based on mass and dimensional measurements, we obtained an average density of 18.8 g/cc (±0.7%) for the W–1%La material.

DShG-200 Be samples with nominal dimensions (12 mm long, 12 mm wide, 5 mm thick) were tested. Based on mass and dimensional measurements, we computed an average density of 1.84 g/cc (±0.3%) indicating that the Be was essentially fully dense.

The irradiated Be samples consisted of both Brush Wellman S65C and Kawecki PO Ductile (DB) Be material. Each specimen was approximately half of a flat tensile test specimen (about 0.88 cm^2 surface area) that was irradiated either in the High Flux Isotope Reactor (HFIR) at Oak Ridge National Laboratory (ORNL) or in the High Flux Beam Reactor (HFBR) at Brookhaven National Laboratory (BNL). Four S65C samples were irradiated in HFIR at nominal irradiation temperatures of 108, 200, 237 and 275 °C to a fast neutron (>0.1 MeV) fluence of 8.33×10^{20} n/cm^2. DB specimens were irradiated in HFBR at 300 °C to fast neutron fluences from 5×10^{19} to 1×10^{21} n/cm^2. One S65C sample was irradiated in HFBR at 300 °C to a fluence of 2×10^{20} n/cm^2.

2.2. Steam oxidation experimental system

Chemical reactivity experiments were conducted with a system comprising a steam generator, a quartz reaction chamber surrounded by a tube furnace, steam condensers, in-line cryotrap, gas analysis instrumentation and an ethylene glycol trap at the terminus of the process line [11,12]. Steam (2500 std-cc/min, 0.84 atm), introduced upstream from the sample furnace, reacted with the hot specimen inside the quartz reaction chamber and was condensed downstream from the sample furnace. Argon carrier gas (100 std-cc/min, 0.84 atm) was used to sweep reaction gases from the reaction chamber through the process line for on line measurements with a mass spectrometer. Oxidation kinetics were monitored by measurements of H_2, CO, and CO_2 concentrations in the Ar carrier gas. Total quantities of the reaction gases were computed by integrating the mass spectrometer data. Average generation rates for each reaction gas were derived as the total gas quantity generated divided by the steam exposure time and the initial geometric surface area for the sample. A microbalance with a precision of 0.1 mg was used to measure the specimen mass before and after testing. Based on the reaction mechanisms, these weight-change measurements provided a second approach to obtain the total quantities of reaction gases generated in experiments for Be and CFC samples. Weight-change measurements could not be used for this purpose in tungsten experiments because of weight loss from mobilization of volatile tungsten oxides.

3. Measurements and results

3.1. CFC material

Chemical reactivity experiments were performed for the NS31 and NB31 CFC samples exposed to steam at temperatures from 800 to 1100 °C. The weight-loss and mass-spectrometry data provided a good correspondence between the average carbon reaction rates at different test temperatures and the corresponding average generation rates for H_2, CO and CO_2. Because H_2 generation in our experiments resulted both from the primary reaction ($H_2O + C \rightarrow CO + H_2$) and from secondary reaction ($H_2O + CO \rightarrow CO_2 + H_2$) [4,5,17], we present here average hydrogen generation rates derived from the carbon weight-loss data. Fig. 1 compares Arrhenius plots of NS31 and NB31 results to previous measurements: (1) GraphNOL N3M graphite tested at 1000–1700 °C [2,3], (2) three different CFCs (Dunlop, FMI-HDFG, FMI-4D) tested at 1100 and 1300 °C [2,3], (3) 2D CFC Aerolor A05 [4,5], and (4) isotropic graphite ETP-10 and a CFC identified as MFC1 [6]. Arrhenius expressions are given in the figure for least squares fits to the N3M data (N3M-F1 and N3M-F2) and for fits to the 1000 and 1100 °C NB31 and NS31 data (NB31-F1 and NS31-F1). Units for the pre-exponentials are ($l/m^2\,s^{-1}$) and the activation energy is in J/mol. The pre-exponentials for NB31 and NS31 can be converted to ($l/g\,s^{-1}$) by using a geometric specific area of 4.30×10^{-4} m^2/g. The NB31 and NS31 Arrhenius fits are extrapo-

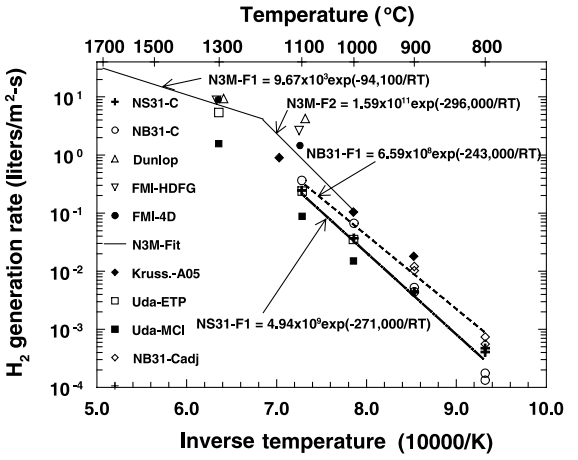

Fig. 1. Hydrogen generation from reaction of graphite with steam.

lated to the lowest test temperature of 800 °C. All other data are shown as discrete data points.

We observe differences in the magnitudes and temperature dependence of the average hydrogen generation rates for NS31 and NB31. On the Arrhenius-type plot, the NS31 data exhibit nearly linear temperature dependence from 1100 to 800 °C whereas the NB31 data show a significant departure from linear behavior at the two lowest test temperatures. For NB31, this deviation in chemical reactivity at 900 and 800 °C is due to much lower burn-off conditions (0.06 and 0.002 kg/m^2, respectively) for these test samples. As discussed by others [4,5,17], chemical reactivity varies significantly for porous carbon materials and becomes relatively stable only after sufficient burn-off (>0.2 kg/m^2) is achieved. The data identified as NB31-Cadj correspond to 800 and 900 °C NB31 test data that have been adjusted upward to correspond to a higher burn-off condition that is consistent with the 1000 and 1100 °C data. Adjustment factors were derived from the burn-off dependent, carbon reactivity data presented by Krüssenberg et al. [4]. The adjusted NB31 data are consistent with the linear fit to the higher temperature data. A linear fit to the NB31 data (both high temperature data points and the adjusted data points) yields an activation energy that is about 6% higher than that for the fit only to the high temperature data. The NS31 data do not exhibit the expected trend at low temperatures, possibly because of the influence of the infiltrated Si. Steam interaction with Si and C in NS31 may contribute to additional reactive gases or catalytic enhancement of carbon chemical reactivity at the lowest test temperatures [5]. In general, the presence of the Si results in a reduction of chemical reactivity by about a factor of 2 for these CFCs.

H_2 generation rates for NS31 and NB31 were about a factor of 2 less than data for the isotropic graphite, N3M, and nearly a factor of 10 less than data for the CFCs, DUNLOP, FMI HDFG and FMI 4D at comparable test temperatures. The differences in absolute H_2 generation rates for NS31 and NB31 compared to the previous data are attributed to material property differences such as density and porosity and to differences in experimental test conditions such as steam flow velocities and gas measurement techniques. Steam flow rates in previous INEEL tests [2,3] were about one order of magnitude higher than for the NB31 and NS31 experiments.

Average H_2 generation rates of NB31 were about 50–70% less than the rates derived from the data reported by Krüssenberger et al. [4], about 40% greater than the results observed by Uda et al. [6] for ETP-10 isotropic graphite but significantly greater than the Uda data for the 2D CFC, MCI. Activation energies derived for the NS31 and NB31 data were comparable to the nominal value of 270 000 J/mol reported by Uda et al. [6] but somewhat greater than the value 217 000 J/mol reported by Krüssenberg et al. [4]. These activation energies are indicative of steam penetration and chemical reactivity at sites within the porous carbon structure via the reaction $H_2O + C \rightarrow CO + H_2$ [17]. Differences between these data are attributed to differences in sample type and experimental test conditions.

3.2. Tungsten material

Chemical reactivity experiments were performed on the W–1%La samples exposed to steam at temperatures ranging from 550 to 1000 °C. Fig. 2 shows Arrhenius plots of the average H_2 generation rates for the W–1%La samples and compares these rates to previously published data for a 95% tungsten alloy [7] and tungsten welding rods with 1.5–wt% La_2O_3 [8]. Arrhenius

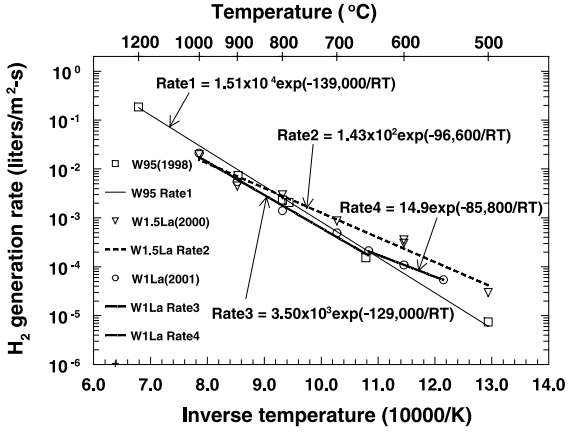

Fig. 2. Hydrogen generation from reaction of tungsten alloy with steam.

expressions were derived from least-squares fits to the different data sets, with identifications given in the figure legend. The W–1%La alloy data are in reasonable agreement with the 95% W alloy data (W95) and the W weld rod data (W1.5La) for temperatures above 650 °C. Below 650 °C, both the W–1%La and W-weld rod data are higher than the 95% W alloy data. We suspect that chemical reactivity for these materials at the lowest test temperatures is affected by differences in material composition and surfaces. Differences in experimental test conditions for the present experiments compared to the previous ones (e.g., steam flow rates, orientation and heating method for the test samples, gas measurement technique) could also contribute to the observed differences in the hydrogen generation rates.

3.3. Unirradiated beryllium

Chemical reactivity experiments were performed on the DShG-200 Be samples exposed to steam at temperatures ranging from 500 to 900 °C. Essentially no H_2 was observed during tests of DShG-200 Be at 500 and 550 °C. Our previous oxidation studies of Be in steam showed parabolic oxidation behavior for temperatures at and below 600 °C. This oxidation behavior was very sensitive to the surface conditions of the samples. Therefore, we attribute the absence of a hydrogen signal at test temperatures of 500 and 550 °C for DShG-200 Be to a pre-oxidized surface layer that was protective in character. For test temperatures above 550 °C, average H_2 generation rates were derived from mass-spectrometer measurements and from mass-change measurements. Fig. 3 shows Arrhenius plots of the average H_2 generation rates (INEEL01-WG, -G) that were derived from the weight-gain (-WG) and mass-spectrometer gas (-G) measurements for the DShG-200 Be samples. These rates are compared to previously published data for fully dense, consolidated powder metallurgy (CPM) Be, {(INEL92-WG, -G) [9], (INEL-96-WG1, -G1) and (INEL-96-WG2, -G2) [11,12], and (TRW65) [10]}. In general the data for DShG-200 Be are in good agreement with the results of the previous studies. Arrhenius expressions in the figure correspond to least-squares fits to the experimental data in three temperature regions: 1200–900 °C, 830–600 °C and 600–450 °C. In the low temperature regime, the experimental data show considerable scatter primarily because the steam-reactivity behavior is very sensitive to the surface conditions of the samples. Because of this, the lowest data points at 600 °C were excluded from the least-squares fit and the Rate1 expression provides a general trend for the average hydrogen generation rates below 600 °C.

3.4. Irradiated beryllium

Steam oxidation experiments were performed at 600–800 °C for S65C samples irradiated to a fast neutron fluence of 8.33×10^{20} n/cm^2. In addition, one steam oxidation experiment was performed at 700 °C for a Kawecki PO ductile Be sample (DB20) that was irradiated to a fast neutron fluence of 1×10^{21} n/cm^2 and subsequently annealed at 1000 °C prior to the chemical reactivity experiment. Average hydrogen generation rates for these experiments (INEEL001IRG, -WG) are presented in the Arrhenius plots of Fig. 4, along with the results from previous studies: (INEL92-G, -WG), for fully dense CPM-Be discs [9]; (INEL92Porous-G) for low density (86%TD) CPM-Be discs [13]; (INEL96-G2, -WG2), for fully dense CPM-Be cylindrical specimens [11,12]; (INEL96IR-G1, -WG1), for high-fluence (5×10^{22} n/cm^2) CPM-Be cylinders [14]; and (INEEL97IRA-G2, -WG2), for high-fluence (5×10^{22} n/cm^2) CPM-Be cylinders that were annealed with slow heat-up ramps to 1100 °C [15]. The rates measured for the low-fluence Be

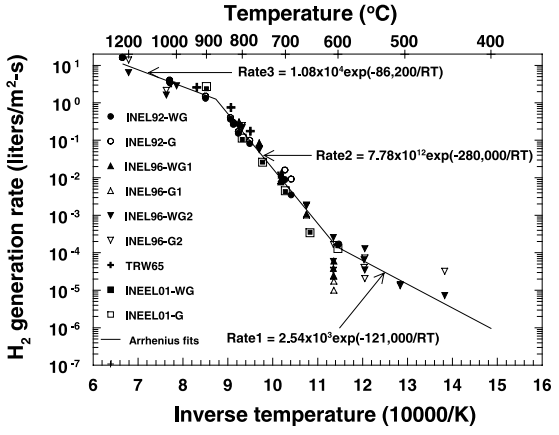

Fig. 3. Hydrogen generation from reaction of beryllium with steam.

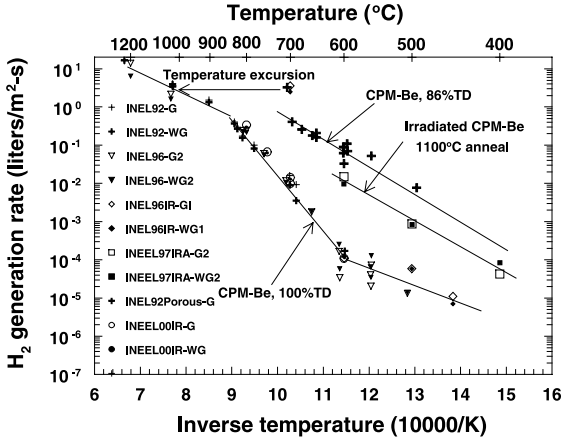

Fig. 4. Hydrogen generation from reaction of steam with unirradiated and irradiated Be.

from the present work are in excellent agreement with the rates measured for unirradiated CPM-Be with 100%TD. In contrast, such agreement is observed for the high-fluence Be [14,15] only for temperatures of 600 °C and below. At a test temperature of 700 °C, the high-fluence irradiated Be experienced a reactivity enhancement and temperature excursion resulting in a hydrogen generation rate more than two orders of magnitude greater than that for unirradiated Be. Furthermore, annealing of the high-fluence Be to 1100 °C produced an enhanced surface area that resulted in H_2 generation rates much higher than those for unirradiated fully dense Be, even for temperatures below 600 °C. In the present experiment for the low-fluence DB20 annealed at 1000 °C, the H_2 generation rate at 700° was in excellent agreement with the unirradiated material. From this we infer that the prior annealing had no affect on the steam–Be reaction rate for the low fluence Be.

4. Conclusions

Hydrogen generation rates were measured for candidate PFC materials exposed to steam. New measurements were reported for NS31 and NB31 CFCs, W–1%La, DShG-200 Be and Be (S65C and Kawecki PO ductile) irradiated to fast neutron fluences between 5×10^{19} and 1×10^{21} n/cm^2, and the results were compared to previously published data.

(1) Steam oxidation rates of NS31 were about a factor of 2 lower than comparable rates for NB31 at 1000 and 1100 °C, and possibly lower for temperatures down to 800 °C. However, the low temperature oxidation behavior for NS31 was higher than that expected for normal oxidation of porous carbon materials under similar test conditions. The data demonstrate that Si impregnation into the CFC material results in reduced oxidation above 900 °C but may contribute to additional reactive gas generation and catalytic enhancement of carbon chemical reactivity below 900 °C.
(2) H_2 generation rates for W–1%La were very consistent with previous steam oxidation measurements for a 95% W alloy at 600 °C and higher. Below 600 °C, the observed rates for W–1%La were higher than for W95 indicating the possible influence of differences in material composition, surface condition and experiment test conditions.
(3) Measured H_2 generation rates for DShG-200 Be at temperatures from 600 and 900 °C are in good agreement with many previous studies for CPM Be.
(4) For Be irradiated to a fast neutron fluence up to 1×10^{21} n/cm^2, the measured H_2 generation rates were in good agreement with steam oxidation data for unirradiated Be at 600–800 °C. In contrast, previous studies for Be irradiated to a fast neutron fluence of 5×10^{22} n/cm^2 demonstrated a significant enhancement in chemical reactivity at a steam exposure temperature of 700 °C because of the development of a surface-connected network of internal porosity.

Acknowledgements

This work was supported partially by the US Department of Energy, Office of Sciences, and by the Forschungszentrum, Karlsruhe GmbH, under the DOE Idaho Operations Contract DE-AC07-99ID13727.

References

[1] C.H. Wu, C. Alessandrini, P. Bonal, H. Grote, R. Moormann, J. Roth, M. Rödig, H. Werle, G. Vieider, J. Nucl. Mater. 258–263 (1998) 833.
[2] G.R. Smolik, B.J. Merrill, S.J. Piet, D.F. Holland, Fus. Technol. 19 (1991) 1342.
[3] G.R. Smolik, B.J. Merrill, S.J. Piet, R.S. Wallace, Evaluation of graphite/steam interactions for ITER, EGG-FSP-9154, Idaho National Engineering Laboratory, 1990.
[4] A.-K. Krüssenberg, R. Moormann, H.-K. Hinssen, M. Hofmann, C.H. Wu, J. Nucl. Mater. 258–263 (1998) 770.
[5] R. Moormann, S. Alberici, H.-K. Hinssen, A.-K. Krüssenberg, C.H. Wu, Adv. Sci. Technol. 24 (1999) 331.
[6] T. Uda, M. Ogawa, Y. Seki, T. Kunugi, I. Aoki, T. Honda, T. Okazaki, N. Nishino, Fus. Eng. Des. 29 (1995) 238.
[7] G.R. Smolik, K.A. McCarthy, D.A. Petti, K. Coates, J. Nucl. Mater. 258–263 (1998) 1979.
[8] G.R. Smolik, R.J. Pawelko, R.A. Anderl, D.A. Petti, Fus. Eng. Des. 54 (2001) 583.
[9] G.R. Smolik, B.J. Merrill, R.S. Wallace, J. Nucl. Mater. 191–194 (1992) 153.
[10] J.L. Blumenthal, M.J. Santy, An experimental investigation of the behavior of beryllium in simulated launch pad abort experiments, TRW Systems, contract no. 82-6211, Sandia Corporation Rep. SCDC-65-1637, 1965.
[11] R.A. Anderl, R.J. Pawelko, M.A. Oates, G.R. Smolik, K.A. McCarthy, Fus. Technol. 30 (1996) 1435.
[12] K.A. McCarthy, G.R. Smolik, R.A. Anderl, R.J. Pawelko, M.A. Oates, R.S. Wallace, Fus. Eng. Des. 37 (1997) 543.
[13] G.R. Smolik, B.J. Merrill, R.S. Wallace, Reactions of porous beryllium in steam, EGG-FSP-10346, Idaho National Engineering Laboratory, July 1992.
[14] R.A. Anderl, R.J. Pawelko, M.A. Oates, G.R. Smolik, K.A. McCarthy, J. Fus. Energy 16 (1997) 101.
[15] R.A. Anderl, K.A. McCarthy, M.A. Oates, D.A. Petti, R.J. Pawelko, G.R. Smolik, J. Nucl. Mater. 258–263 (1998) 750.
[16] S. Brunauer, P.H. Emmett, E. Teller, J. Am. Chem. Soc. 60 (1938) 309.
[17] P.L. Walker Jr., F. Rusinko Jr., L.G. Austin, Adv. Catal. 11 (1959) 133.